frontiers | Frontiers in Manufacturing Technology

TYPE Original Research
PUBLISHED 30 August 2022
DOI 10.3389/fmtec.2022.964450

OPEN ACCESS

EDITED BY
Emel Kuram,
Gebze Technical University, Turkey

REVIEWED BY
Anil Bastola,
University of Nottingham,
United Kingdom
Candice Majewski,
The University of Sheffield,
United Kingdom

*CORRESPONDENCE
O. Ghita,
o.ghita@exeter.ac.uk

SPECIALTY SECTION
This article was submitted to Additive Processes,
a section of the journal
Frontiers in Manufacturing Technology

RECEIVED 08 June 2022
ACCEPTED 25 July 2022
PUBLISHED 30 August 2022

CITATION
Benedetti L, Brulé B, Decraemer N, Evans KE and Ghita O (2022), Evolution of PEKK crystallization measured in laser sintering.
Front. Manuf. Technol. 2:964450.
doi: 10.3389/fmtec.2022.964450

Evolution of PEKK crystallization measured in laser sintering

L. Benedetti[1], B. Brulé[2], N. Decraemer[2], K. E. Evans[1] and O. Ghita[1]*

[1]College of Engineering, Mathematics and Physical Sciences, University of Exeter, Exeter, United Kingdom, [2]Arkema Cerdato, Serquigny, France

The rising popularity of laser sintering (LS) technology has increased by the broadening of available materials for this process. Kepstan 6002 poly (ether ketone ketone) (PEKK) was recently launched as a high-performance polymer grade with a lower processing temperature and unique crystallization kinetics. This study aims to understand the progress of crystallization on samples manufactured throughout the laser sintering process. These results were compared with isothermal and dynamic differential scanning calorimetry (DSC) experiments with different cooling rates. Kepstan 6002 PEKK processed by high-temperature laser sintering (HT-LS) presents a kinetics of crystallization in the order of ~10 times slower than its crystallized samples in the DSC. This result highlights the need for a part-based crystallization investigation rather than isothermal models to describe the crystallization in LS. The transmission electron microscopy (TEM) analysis reveals smaller spherulites in the samples subjected to prolonged cooling times and an almost amorphous structure for the PEKK samples exposed to almost no cooling. This experiment identified the surroundings of laser sintered particles as preferential sites for crystallization initiation, which grows as the particles penetrate the molten layers and spherulites are formed. The slower kinetics of crystallization of Kepstan 6002 PEKK grade improve the adhesion between layers in laser sintering and enable tailoring its properties according to the application. Understanding the relationship between intrinsic material characteristics and the resulting final properties is vital to optimizing the process and controlling the final performance of PEKK for different applications.

KEYWORDS

laser sintering, high-performance polymers, PEKK, crystallization kinetics, crystalline structure

1 Introduction

The Laser Sintering (LS) process enables the free-tooling production of complex geometries with comparable or higher mechanical strength than conventional manufacturing techniques (Bourell et al., 2014). The achievement of higher strength in polymers is usually attributed to the slow cooling of this process (Kruth et al., 2007; Paolucci et al., 2019), in the order of hours as opposed to the seconds or a couple of minutes generally applied to cool injection molded (IM), or extruded parts (Zarringhalam

et al., 2006; Athreya et al., 2011; Van Hooreweder et al., 2013; Zhu et al., 2015). The layer-by-layer nature of the LS process, which requires subsequent spreading and melting of the powder in the powder bed, significantly increases the manufacturing time, but it is essential to achieve a fully solid structure with comparable performance to injection molding (IM) (Bourell et al., 2014).

Drummer et al. (Drummer et al., 2019) could detect complete solidification of the LS polymer components at a few millimeters below the surface if the appropriate build chamber temperature is chosen to maintain quasi-isothermal conditions of crystallization. Therefore, they proposed a significantly more efficient LS cooling, in which 15 additional layers of powder of 1.5 mm thickness, equivalent of about 10 minutes of production in total, are already sufficient to solidify the parts with no visible warpage.

Other study (Athreya et al., 2011) reported a comparable degree of crystallinity of IM and LS polyamide 12 (PA12). The microstructure of LS PA12, however, was remarkably different from IM PA12, the latter with spherulites varying from 5 to 10 μm in diameter, while the spherulites of LS PA12 matched the diameter of the particles used for LS, being noticeably broader across XY plane. Similar conclusions were drawn by Zarringhalam et al. (Zarringhalam et al., 2006), in addition to finding larger spherulites for LS PA12 compared to IM PA12, pointed to unmolten particle cores from which crystals were formed. These cores presented a higher melting peak despite having the same crystalline structure (γ form) as the rest of the polymer structure.

In the case of amorphous polymers, such as polycarbonate (PC), the polymer chains remain disorganized regardless of the cooling time and cooling rate of the process. For semi-crystalline polymers in which the kinetics of crystallization is particularly slow, e.g., Kepstan 6002 PEKK, the rate and time for cooling are critical factors in the process because they change the intrinsic properties of the material, i.e., the degree of crystallinity, crystal size, and crystalline structure. In this way, the Kepstan 6002 PEKK grade is fully amorphous when processed by IM but crystallizes in a slow cooling process as LS (Benedetti et al., 2020).

The kinetics of crystallization is determined by the rate of nuclei formation and their rate of growth. The temperature range to which crystallization occurs usually varies from 10°C below the melting temperature (T_m) to 30°C above the glass transition temperature (T_g). Near the T_m, chain realignment is facilitated by the reduced viscosity of the liquid phase and the free energy increase within the system. These factors are so strong that any potential nuclei are disrupted before growth occurs, increasing the time for polymer nucleation and the formation of spherulitic crystallites. On the other hand, temperatures close to T_g significantly reduce chain mobility and increase liquid phase viscosity. These factors decrease the chances for nuclei growth (Hoffman and Lauritzen, 1961; Motz and Schultz, 1989; Van Krevelen and Te Nijenhuis, 2009).

Motz and Schultz (Motz and Schultz, 1989) investigated the solidification and kinetics behavior of poly (ether ether ketone) (PEEK). They concluded that at slow cooling rates of 1.25°C min^{-1}, PEEK starts crystallizing at 315°C and the crystallization occurs at a narrow temperature range of 10°C. In a fast solidification of 160°C min^{-1}, crystallization process starts at 285°C, 30°C lower than at slow cooling rates. Interestingly, the cooling rate seems to have a limiting effect on the degree of crystallinity, possibly due to the high nucleation density of this polymer. Cebe and Hong (Cebe and Hong, 1986) confirmed this phenomenon and found a degree of crystallinity of about 29% for PEEK cooled from the melt at cooling rates varying between 10 and 160°C min^{-1}. Nonetheless, Motz and Schultz (Motz and Schultz, 1989) highlighted that a faster cooling than the polymer's rate of crystallization might lead to incomplete crystallization, affecting final crystal morphology.

The crystallization kinetics and crystalline structure of semi-crystalline polymers processed by LS were recently investigated and compared with IM for PA12 (Ajoku et al., 2006; Zarringhalam et al., 2006; Van Hooreweder et al., 2013), PA11 (Leigh, 2012), PP (Zhu et al., 2015), PBT (Arai et al., 2017) and PAEKs (Wang et al., 2016). All the studies revealed different structures varying with the process, which directly affected final mechanical properties. The degree of crystallinity in LS is usually high, and the crystal structure, i.e., spherulites, smaller (Athreya et al., 2011). Smaller spherulites are preferred as crack propagation is delayed. The number of nuclei and the cooling rate must be high (Van Krevelen and Te Nijenhuis, 2009) to obtain small spherulites. Regarding mechanical properties, the increase in the percentage of crystallinity results in higher strength and modulus but significantly lower elongation (Zhu et al., 2015).

According to Kruth et al. (Kruth et al., 2007), the slow cooling in LS should allow time for full particle coalescence and bonding as well as chain rearrangement for crystal formation and growth. For polymers with high crystallization kinetics, bonding can be compromised if the preceding layers do not remain in the molten state. Such is the case of POM polymer reported by Drummer et al. (Drummer et al., 2010), which due to the high kinetics of crystallization, failed in a brittle fashion despite successfully consolidated (Drummer et al., 2010).

The increase in the mechanical strength often follows a significant decrease in the elongation at break, leading to brittle and unpredictable failure. In a previous study (Benedetti et al., 2020), elongation was increased by varying the cooling time in LS of PEKK material. The change in cooling time directly affected the degree of crystallinity of PEKK, which resulted in improved elongation at break while ultimate mechanical strength was slightly compromised.

Besides the mechanical properties, the LS process may also affect crystallization and the spherulitic formation in semi-crystalline polymers. As opposed to the full melting of the polymeric structure, the LS process applies heat to particular

regions of the powder bed, which may trigger different forces to promote coalescence. Previous studies (Zarringhalam et al., 2006; Stichel et al., 2017) have also highlighted the presence of unmolten particle cores resulting from the LS process. Furthermore, the cooling rate of this process is unique, being dynamic but significantly slow. Thus, current crystallization models can lead to the incorrect fitting of the crystallization kinetics occurring in LS. As a result, it is crucial to consider material-process interaction when investigating the kinetics of crystallization.

This study takes a different approach to the traditional methods of investigating the progress of crystallization in a manufacturing process. Rather than measuring crystallinity on a range of isothermal and dynamic thermal studies, we experimentally investigated the kinetics of crystallization as parts are being formed in high-temperature laser sintering (HT-LS). The crystalline structure of the LS specimens is analyzed under transmission electron microscopy (TEM) and differential scanning calorimetry (DSC) techniques to understand and therefore correlate the mechanical properties achieved at different cooling times with the intrinsic crystallization behavior of PEKK manufactured in HT-LS.

2 Experimental section

2.1 Material

This study used Kepstan 6002 PEKK powder supplied by Arkema (Arkema, 2019), also known by the commercial name of PEKK HPS1. This PEKK grade has a T_g of 160°C, and a T_m of ~300°C.

2.2 Manufacturing procedure of LS samples of different crystallinities

The experimental method designed for this study investigates the crystallization of Kepstan 6002 PEKK in LS by varying the cooling time throughout the build. The build was produced in a high-temperature EOS *P* 800 system in the reduced chamber configuration (Berretta et al., 2015). From a previous study (Benedetti et al., 2019a) developed with Kepstan 6002 PEKK, the best combination of laser parameters used to improve the mechanical performance of LS parts applies a total energy density of 23.5 mJ×mm^2 per layer. The bed temperature (T_{bed}) was calculated from the minimum of the first derivative of the heating segment in the DSC (Berretta et al., 2016), and the building platform temperature (T_{bp}) was selected as the average between the temperature at which kinetics of crystallization is the highest and the melting peak of PEKK. These temperatures were previously explored material in (Benedetti et al., 2020) and correspond to, respectively, 292 and 190°C.

The build setup comprises sixteen groups of specimens stacked on top of each other in Z orientation (see Figure 1). Each group consists of ten ISO 527–2-1BA specimens produced in X orientation, subjected to specific cooling times based on their height along z orientation. The groups followed a sequential order from the bottom (group 1) to the top (group 16). The experiment setup took approximately 10.75 h to complete, excluding the pre-heating stage. Following the manufacture of group 16, the build was immediately interrupted so that no empty layer of powder was applied to the top. The part cake with all the specimens (group 1 to group 16) was removed from the system. As the height along z orientation varied for each group of specimens, the cooling time was tailored accordingly. The specimens were quenched in water at approximately 15°C. The part cake was broken into small parts to help with homogeneous cooling and allow the quick penetration of water. After approximately 12 hours of cooling, the specimens were left to drying for 12 h before being taken to test. Figure 1 summarizes the build configuration and the results previously achieved that are relevent in the present study. More information on the build setup can be found in (Benedetti et al., 2020).

In a previous study (Benedetti et al., 2020), this methodology significantly improved the elongation at break of HT-LS PEKK, which was associated with the level of crystallinity obtained for each group of specimens subjected to different cooling times (Benedetti et al., 2020). In addition to the degree of crystallinity, the structure of the material may be affected by the interruption of the cooling process. In this study, we aim to continue to investigate the kinetics

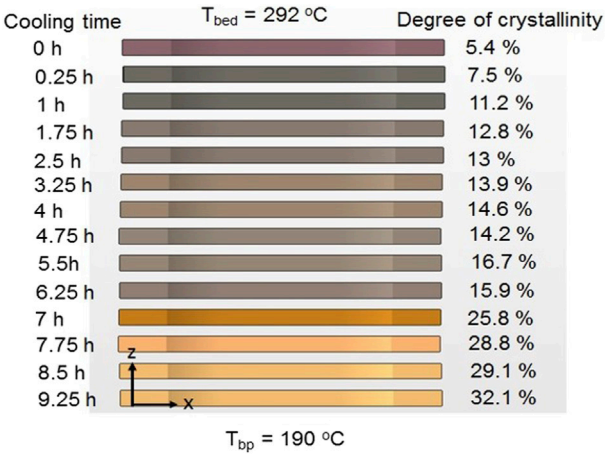

FIGURE 1
Crystallization build setup in x-z plane indicating T_{bed}, T_{bp}, and the cooling time applied for each group of specimens (left side of the specimens). The average degree of crystallinity was measured using WXRD, and is indicated on the right. The color of the specimens attempted to match their level of crystallinity from amorphous to semi-crystalline PEKK.

of crystallization in LS and the resulting changes in the crystalline structure, in respect to arrangement and size. These information will lead to a broader understanding of the effect of processing conditions in material behavior.

2.3 Sample characterization after manufacture

2.3.1 Differential scanning calorimetry (DSC)

The crystallization properties of powder samples of Kepstan 6002 PEKK were analyzed in dynamic and isothermal conditions. The experiments were performed in a Mettler Toledo 821e/700 DSC and evaluated with the assistance of the Star^e SW 12.10 software (Mettler Toledo, 2011).

The powder samples subjected to dynamic conditions were heated up to 400°C (above PEKK T_m) and cooled to room temperature at the following cooling rates: 1°C×min^{-1}, 1.5°C×min^{-1}, 2°C×min^{-1}, and 5°C×min^{-1}. For the isothermal tests, powder samples were heated at 20°C×min^{-1} from 25°C to 380°C, then quickly cooled at 80°C×min^{-1} to the chosen isotherm temperature. The quick cooling was added to prevent crystallization prior to the isotherm step. The isotherm was maintained for 120 min to enable full crystallization, and was followed by cooling at 20°C×min^{-1} until reaching 25°C. The isotherm temperatures varied from 200°C to 270°C at an interval of 10°C, as this is the range at which PEKK crystallizes. Both isothermal and dynamic tests used a nitrogen flow rate of 50 ml min^{-1}. For the isothermal tests, the samples were placed in aluminum pans with a volume of 100 μL. For the dynamic tests, the volume of the aluminum pans was 40 μL.

2.3.2 Transmission electron microscopy

A JEOL JEM-1400 electron microscope was used in the transmission mode to investigate the crystal structure of Kepstan 6002 PEKK manufactured by LS. Samples of the specimens subjected to cooling times of 10, 5.5, and 0 h (almost amorphous specimens) were compared with the TEM images of PEKK processed at standard condition (same energy density but different T_{bp} and cooling cycles).

The LS specimens were cut into thin sections of approximately 90 nm with the assistance of an RMC POWERTOME PC Ultracut. The sections taken for analysis were removed from the middle of the specimens. The imaging analysis was conducted at a voltage of 120 kV and 77.2 μA using an ES 100 W CCD digital camera (Gatan, Abingdon, UK). Images were captured at different magnifications varying from 3,000× to 250,00×.

3 Cooling in high-temperature laser sintering

Previous studies (Benedetti et al., 2020) estimated the average cooling during the LS process to be approximately 0.5°C×min^{-1}. Although it is currently challenging to access the temperature profile at high temperatures and at punctual places in the powder bed, it is possible to divide the process into three main cooling stages. The first cooling stage is caused by the removal of the laser beam from the molten area and the subsequent contact of the molten material with T_{bed} (Benedetti et al., 2019b). Following this quick cooling, in the order of milliseconds, a longer cooling occurs during manufacturing, while new parts are built, and the already sintered specimens in the bottom of the build are gradually cooling down. The second stage has the slowest cooling of all the stages and is entirely dependent on the selection of T_{bed} and T_{bp}. As the crystallization range for Kepstan 6002 PEKK is located between these temperatures, this stage is dominant on the resulting crystallinity of HT-LS PEKK parts. Finally, after build completion, the system applies a standard cooling phase that varies with the total height of the build in the z-direction and the volume and distribution of the parts across the build. The cooling rate is unknown in this stage, however, the system switches off below the glass transition temperature (T_g) to accelerate cooling.

Chen et al. (Chen et al., 2020) described the crystallization in LS as a complex periodic process divided in a dynamic crystallization stage, promoted by the coating of a sintered layer of cold powder, and a quasi-static isothermal crystallization stage led by the maintenance of T_{bed} in LS. They highlight that such cooling cannot be compared with the DSC condition, especially because of the first stage, which significantly affects the sintering window if T_{bed} is not quickly recovered. This study, however, does not account for a T_{bp}, a third factor that may result in a dynamic cooling with a different rate from the first stage associated with the cold powder coating.

Drummer et al. (Drummer et al., 2019) experimentally measured the powder bed temperature and the temperature within deeper layers in z-direction as the LS process progresses. The authors found out that the coating of a new layer induces a dynamic process, dropping the temperature by 18°C for the case of PA12, and therefore leading to crystallization acceleration. This experiment, however, is not feasible for HT-LS systems and does not account for a second temperature, T_{bp}.

The success of LS highly depends on providing sufficient time for full particle coalescence and bonding, and chain rearrangement for crystal formation and growth (Kruth et al., 2007). The layer bonding is improved by chemically modifying the polymer to delay solidification and slow down the kinetics of crystallization (Dupin et al., 2012). This approach was taken to produce the Kepstan 6002 PEKK (Arkema, 2019) supplied by Arkema. When processed by conventional manufacturing techniques, e.g., injection molding and extrusion calendaring, Kepstan 6002 PEKK does not have sufficient time to crystallize; therefore, it remains in the amorphous state. The slow cooling in LS, however, promotes its crystallization. The approach to analyzing the effect of slow cooling is usually the performance of multiple isothermal tests (Tardif et al., 2014; Chen et al., 2020).

However, LS does not seem to present an isothermal cooling but a dynamic one with different cooling rates varying as the stage in the process changes.

4 Results and discussions

4.1 Kinetics of crystallization in LS

The slow kinetics of crystallization of Kepstan 6002 PEKK was firstly investigated using the DSC in dynamic and isothermal conditions (Section 2.3.1). The relative volumetric crystallinity of the powder samples subjected to DSC is presented in Figure 2.

The PEKK powder exposed to isothermal crystallization at 220°C, 230°C and 240°C is fully crystalline in less than 30 min; the same is found for the dynamic curves below 1°C×min^{-1}. The crystallization rate gradually decreases for temperatures below and above this range and is the longest at the isothermal temperature of 270°C, in which chain mobility is high, but nuclei formation is the lowest. For the curve with a dynamic rate of 1°C×min^{-1}, the time taken to achieve full crystallization is almost 48 min, while at 5°C×min^{-1} the time taken to complete crystallization is 14 min.

The dynamic and isothermal PEKK curves were compared with the data obtained when crystallizing PEKK in LS, measured using the build experiment described in Section 2.2. For this analysis, the group with the maximum level of crystallinity (9.25 h, 32% of crystallinity, according to (Benedetti et al., 2020)) was considered to have a relative volumetric crystallinity of 100%, i.e., the maximum possible crystallinity obtained with the LS of PEKK. The degree of crystallinity of the LS specimens was measured under wide-angle x-ray diffraction (WXRD) and was presented in Figure 1. From 9.25 to 5.5 h of cooling, the level of crystallinity is reduced by half, from 32.1 ± 0.6% to 16.7 ± 3.2%. Further discussion on the topic can be found in (Benedetti et al., 2020).

Figure 3 presents some isothermal and dynamic curves from DSC samples of PEKK against experimental data obtained from LS of PEKK measured using WXRD (solid black line). The time to achieve the same relative volumetric crystallinity for the LS process is in the order of 10 times longer than the isothermal and dynamic crystallized samples. Recent models used to describe crystallization in LS (Paolucci et al., 2018; Paolucci et al., 2019) were validated using isothermal profiles taken from flash DSC data, but based on the results of Figure 3, they do not seem to correspond with the actual crystallization in LS. In Figure 3, there is a striking difference between the kinetics of crystallization of the DSC samples and the crystallization of LS specimens obtained at different cooling times. A small part of this difference can be explained by the assumptions considered to develop the LS curve. These assumptions include the method applied to compute volumetric crystallinity, i.e., DSC versus WXRD, the process in LS being quasi-static but not isothermal or dynamic (Chen et al., 2020), the extra few minutes to remove the build from the system and interrupt crystallization, the variance in the calculation of crystallinity using WXRD and the errors originated from the sudden interruption of the cooling in the build.

Drummer et al. (Drummer et al., 2019) evaluated crystallization of PA12 in LS and concluded that the cooling time applied can be significantly reduced, as 50% of the total crystallinity is achieved after 22 min of processing if the usual building chamber temperature of 168°C is selected. They agree with this study in respect to LS not being able to be modeled as an

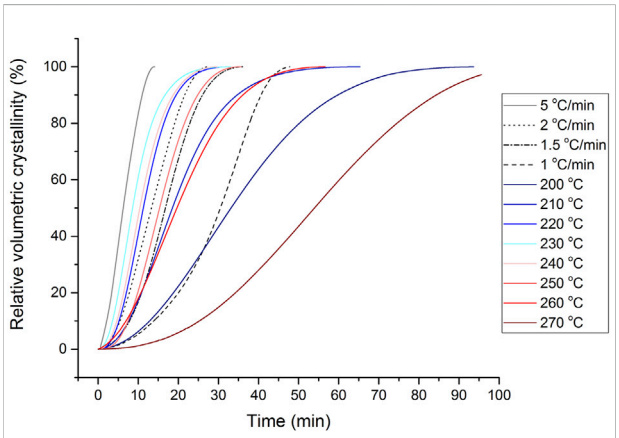

FIGURE 2
Relative volumetric crystallinity of Kepstan 6002 PEKK subjected to isothermal (colored lines) and dynamic (black lines) cooling.

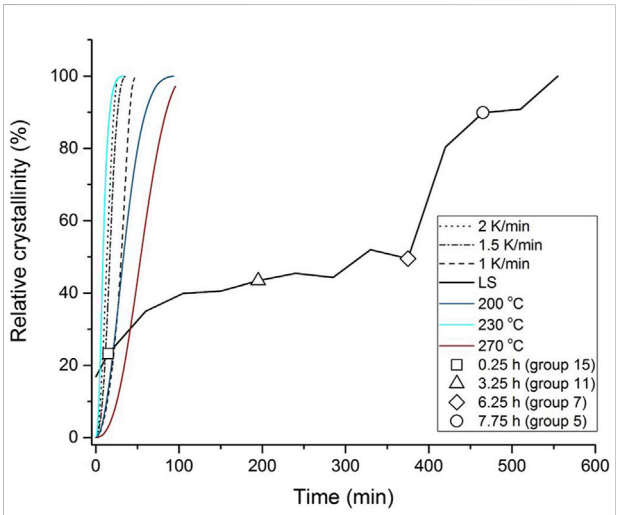

FIGURE 3
Relative crystallinity of isothermal and dynamic crystallized Kepstan 6002 PEKK samples compared with the evolution of crystallinity in the LS process. The time to crystallize the specimens of a few specific groups is highlighted in the LS line by points of different shapes.

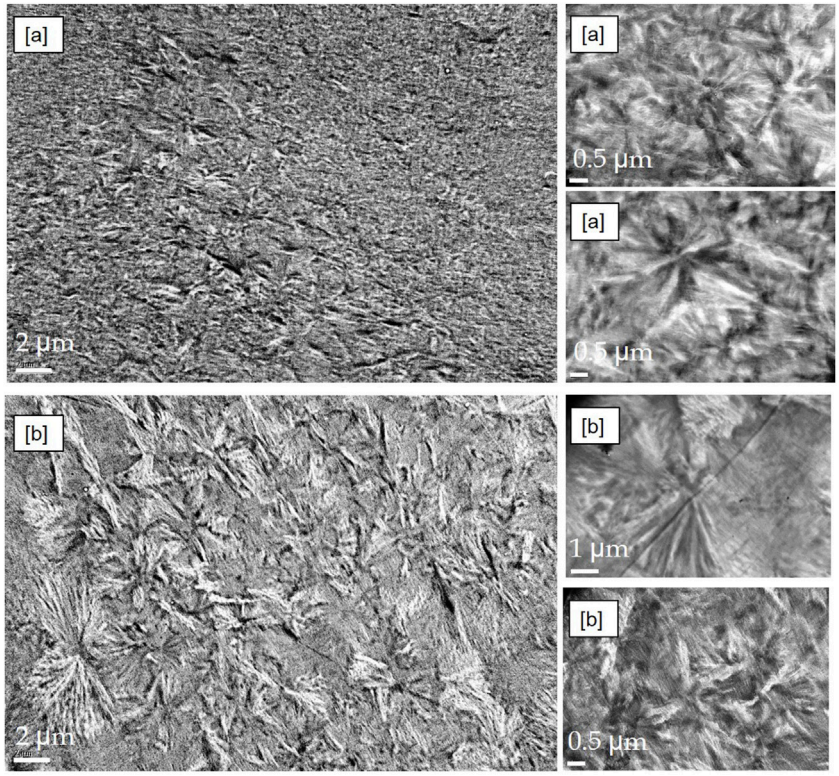

FIGURE 4
TEM images of LS specimens manufactured at T_{bp} of **(A)** 265°C and **(B)** 286°C at different magnifications shown by the scale bars. The spherulites obtained at T_{bp} of 265°C are overall smaller and vary between 2.8 and 5.8 μm in diameter, while the spherulites resulting from a T_{bp} of 286°C are larger and vary between 3.7 and 7.5 μm in diameter.

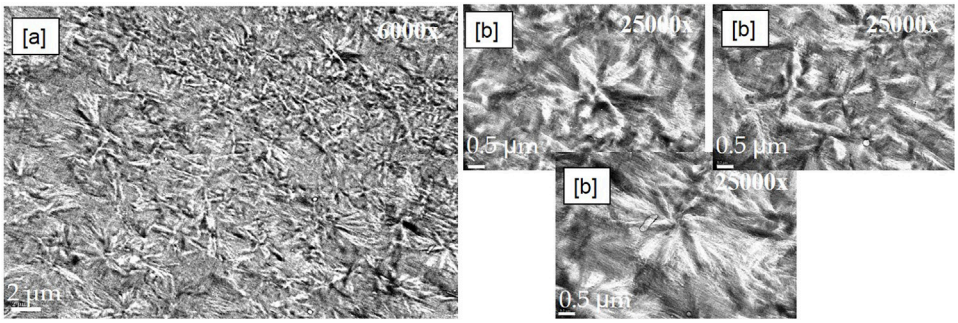

FIGURE 5
PEKK spherulites formed after 10 h of cooling in HT-LS. **(A)** General morphology of the spherulites and **(B)** magnified images of individual spherulites. The spherulites are homogeneously distributed at varying sizes from 5.4 to 5.7 μm in diameter.

isothermal process, and mentioned that this assumption is only valid for the uppermost layers but must be reconsidered for the complete building evaluation.

In this study, the crystallization in HT-LS clearly differs from the DSC profiles, isothermal or dynamic. Similar findings were stated by Yi et al. (2022). This significant difference highlights the complexity of the LS process, which as opposed to the melting and cooling promoted in the DSC, is affected by the punctual application of heat by the laser (Zarringhalam et al., 2006), and the complicated heat transfer taking place between the sintered

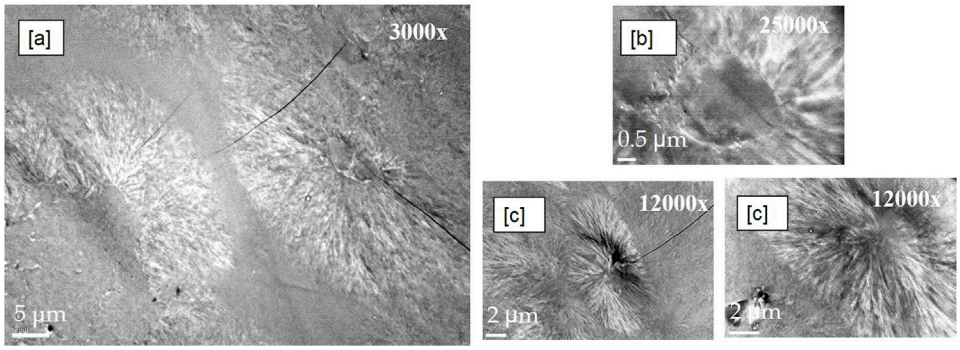

FIGURE 6
PEKK spherulites formed after 5.5 h of cooling in HT-LS. **(A)** General morphology of the spherulites, **(B)** magnified images of the core structure, **(C)** magnified images of the spherulites' structure. The spherulites start growing from particle cores.

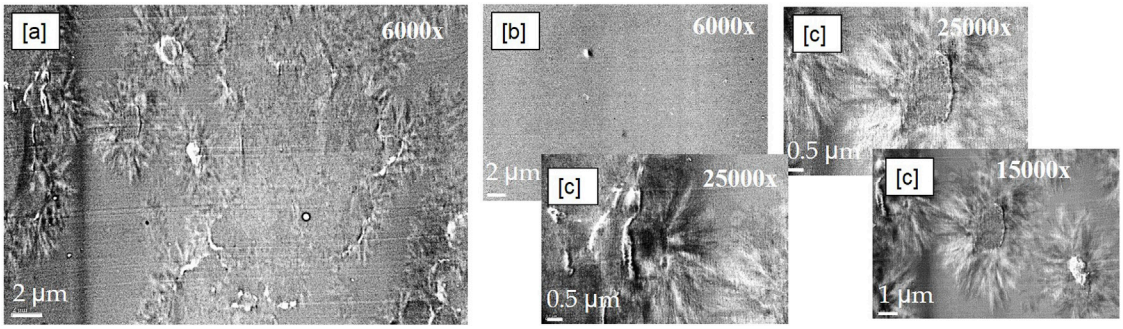

FIGURE 7
PEKK spherulites formed with minimal LS cooling time approaching 0 h **(A)** General morphology of the crystallized region, **(B)** image of the amorphous region, and **(C)** magnified images of the particle cores penetrating the molten PEKK structure. The quenching was not enough to prevent full crystallization.

layers, which can lead to recrystallization (Drummer et al., 2019; Chen et al., 2020). These variances may be aggravated for polymers with slow kinetics of crystallization, such as Kepstan 6002 PEKK, in which an induction time may be required to start crystallization, therefore delaying it by several minutes depending on the processing temperatures selected.

4.2 Crystal structure formation

Samples of the specimens subjected to cooling times of 10, 5.5, and 0 h were taken to TEM analysis and compared with the TEM images of PEKK processed at standard condition. The standard condition corresponds to a laser power of 12 W, a scanning speed of 2,550 mm s^{-1}, and a scanning space of 0.2 mm, resulting in an energy density (ED) of ~23.5 mJ mm^{-2}. The optimized bed temperature T_{bed} (top temperature) is 292°C, and two different building platform temperatures T_{bp} (bottom temperature) were tested: 265 and 286°C. All the specimens were manufactured in X orientation. The mechanical properties of the PEKK specimens produced at the standard condition are available in (Benedetti et al., 2019a); their TEM images are shown in Figure 4.

The average diameter of the spherulites exposed to T_{bp} of 265°C varies from 2.8 to 5.8 μm, while at T_{bp} of 286°C their average diameter increases to between 3.7 and 7.5 μm. These findings agree with the theory of crystallization, in which more nuclei are stabled at temperatures near the maximum rate of crystallization. Therefore, less space is left for growth as they collide with each other. At higher temperatures (T_{bp} of 286°C), fewer nuclei are stable, and the chains are freer to move. Hence

the spherulites achieve a larger diameter (Van Krevelen and Te Nijenhuis, 2009).

The TEM images of the specimens produced with controlled cooling of 10, 5.5, and 0 h are presented in Figures 5–7. The crystalline structure achieved with 10 h of cooling (Figure 5) resembles those obtained when cooling PEKK at standard HT-LS conditions, as shown in Figure 4. When interrupting the cooling at 10 h, the spherulites' size varies between 5.4 and 5.7 μm, which corresponds to intermediate diameters of the spherulites obtained at the standard cooling condition of T_{bp} of 265 and 286°C. A possible explanation for the narrower variation in the diameter of the spherulites achieved with 10 h of cooling is the uniform cooling obtained during manufacture, which is slower and more controlled than when the HT-LS system goes through the standard cooling cycle set by the software.

At 5.5 h of cooling (Figure 6), the PEKK specimens present both crystalline and amorphous regions. The crystalline structures are radially distributed and seem to have initiated around the particles' cores. Zarringhalam et al. (Zarringhalam et al., 2006) observed a similar phenomenon in the LS of recycled PA12. In their case, the DSC revealed a higher T_m for the cores than the rest of the structure. Further investigation showed that such cores resulted from already used powder, i.e., recycled powder, which had its structure modified and did not melt the same as the virgin material but remained unmolten. These unmolten particles triggered heterogeneous nucleation. In our experiment, however, only virgin PEKK particles were used. Furthermore, the cores with a different structure are not present in the specimens subjected to 10 h of cooling, which are part of the same build. A closer investigation of the images presented in Figure 6 reveals crystalline regions located in the surroundings of particles penetrating the molten material (Drummer et al., 2019). At 5.5 h of cooling, some spherulites have been formed (Figure 6C), and others (Figure 6A) are in the process of crystallizing, in which the particles' cores remain visible and the crystallization sites are growing around them (Figure 6B). Interestingly, the formed spherulites at 5.5 h of cooling assume a different structure from those exposed to 10 h of cooling. This difference can be explained by the incomplete crystallization at 5.5 h due to the sudden interruption of cooling while the polymer chains were still being arranged in the structure.

The TEM images of the specimens approaching 0 h of cooling are shown in Figure 7. PEKK assumes an essentially amorphous structure (Figure 7B), although crystalline regions are observed around the particle cores. A few magnified images of the particle cores penetrating the molten material are shown in Figure 7C. Due to the rapid cooling, solidification took place as crystallization initiated, and no complete spherulites could be formed before quenching. As observed for PEKK exposed to 5.5 h of cooling, only primary crystallization was formed for the LS PEKK subjected to abrupt quenching.

The spherulites of PEKK obtained with HT-LS usually vary between 3 and 7 μm in diameter (Figure 4). By interrupting the standard cooling cycle in HT-LS, incomplete structures are formed, which start from the surrounding sites of the particles penetrating the molten layers. The molten particles from the sintered region start penetrating the molten layers of material while crystalline regions are formed around them. As the cooling time increases, the crystal structures grow, although completely amorphous regions are still present unless sufficient time is given for full crystallization.

The LS particles act as sites for heterogeneous nucleation to occur, accelerating crystallization. However, the level of crystallinity in the LS process is similar to several conventional manufacturing techniques if sufficient time for full crystallization is given. The main advantage of LS, therefore, is the ability to easily tailor the degree of crystallinity to attend different application needs (Benedetti et al., 2020).

5 Conclusion

This study monitors the crystallization and crystal structure of PEKK during the cooling stage in HT-LS. Through experimental work, this research provides a deeper understanding of material-process relationship and opens up a range of possibilities for tailoring material properties in HT-LS.

As opposed to previous publications (Amado et al., 2012; Paolucci et al., 2018), the kinetics of crystallization of PEKK is directly influenced by the process, as HT-LS does not follow the same trend obtained with isothermal or dynamic crystallized samples in the DSC. The resulting time to crystallize PEKK specimens in HT-LS is about ten times longer than in the DSC, highlighting that neither isothermal nor dynamic conditions can replicate the cooling inside the HT-LS system, but a part-based crystallization investigation is needed. The striking difference between the kinetics of crystallization in LS and isothermal/dynamic crystallized samples in DSC can be explained by the laser's punctual heat application, which cannot melt the particles fully, and the complex heat transfer phenomenon occurring between the layers during the process.

A close investigation of the LS PEKK microstructure reveals different stages in the crystallization process, with the LS particles acting as sites for nucleation. If the parts are quenched in water as soon after manufacture, most of the structure is amorphous, but crystalline regions are identified surrounding the partially molten particles. As cooling continues, crystallization occurs, and spherulites are observed. At prolonged cooling times, the spherulites achieve between 5.4–5.7 μm in diameter.

Understanding microstructure formation and material properties are crucial for the successful improvement of final

part performance. The control of cooling rate and cooling time change the degree of crystallinity and the diameter of the spherulites, therefore affecting final mechanical properties of HT-LS parts, as previously presented (Benedetti et al., 2020). New systems have been created with integrated post-processing (EOS 3D Printing Technology, 2020; Additive Industries, 2019) to meet the demands for serial production. Rapid cooling (liquid or gas form) could be added to optimize material properties, and therefore apply a similar solution to improve the mechanical performance of polymers with slow kinetics of crystallization.

Data availability statement

The original contributions presented in the study are included in the article/Supplementary Material, further inquiries can be directed to the corresponding author.

Author contributions

LB: Manuscript scope, data gathering, data analysis, manuscript writing and review. BB: Suggestions, scientific knowledge, manuscript review and corrections ND: Suggestions, scientific knowledge, manuscript review and corrections KE: Concept development, suggestions, scientific knowledge, manuscript review and corrections OG: Concept development, suggestions, data analysis and review, manuscript writing, revision, and final corrections.

Funding

The funding comes from a joint collaboration between the University of Exeter and Arkema Chemistry Co. Both parties contributed with knowledge, data, materials, and equipment.

Acknowledgments

The authors would like to acknowledge the financial support of Arkema Innovations Chemistry for this study.

Conflict of interest

The authors declare that the research was conducted in the absence of any commercial or financial relationships that could be construed as a potential conflict of interest.

Publisher's note

References

Additive Industries (2019). *Industrial solutions for metal additive manufacturing.*

Ajoku, U., Hopkinson, N., and Caine, M. (2006). Experimental measurement and finite element modelling of the compressive properties of laser sintered Nylon-12. *Mater. Sci. Eng. A* 428, 211–216. doi:10.1016/j.msea.2006.05.019

Amado, F., Wegener, K., Schmid, M., and Levy, G. (2012). Characterization and modeling of non-isothermal crystallization of Polyamide 12 and co-Polypropylene during the SLS process. *5th Int. Polym. Mould. Innov. Conf.*, 207–216.

Arai, S., Tsunoda, S., Kawamura, R., Kuboyama, K., and Ougizawa, T. (2017). Comparison of crystallization characteristics and mechanical properties of poly(butylene terephthalate) processed by laser sintering and injection molding. *Mat. Des.* 113, 214–222. doi:10.1016/j.matdes.2016.10.028

Arkema (2019). *Kepstan PEKK resins for extremely demanding applications.*

Athreya, S. R., Kalaitzidou, K., and Das, S. (2011). Mechanical and microstructural properties of Nylon-12/carbon black composites: Selective laser sintering versus melt compounding and injection molding. *Compos. Sci. Technol.* 71, 506–510. doi:10.1016/j.compscitech.2010.12.028

Benedetti, L., Brulé, B., Decraemer, N., Davies, R., Evans, K. E., Ghita, O., et al. (2020). A route to improving elongation of high-temperature laser sintered PEKK. *Addit. Manuf.* 36, 101540–101610. doi:10.1016/j.addma.2020.101540

Benedetti, L., Brulé, B., Decraemer, N., Davies, R., and Evans, K. (2019). Mechanical performance of laser sintered poly (ether ketone ketone). *30th Annu. Int. Solid Free. Fabr. Symp.*, 1–14.

Benedetti, L., Brulé, B., Decreamer, N., Evans, K. E., and Ghita, O. (2019). Shrinkage behaviour of semi-crystalline polymers in laser sintering: PEKK and PA12. *Mat. Des.* 181, 107906. doi:10.1016/j.matdes.2019.107906

Berretta, S., Evans, K. E., and Ghita, O. (2015). Processability of PEEK, a new polymer for high temperature laser sintering (HT-LS). *Eur. Polym. J.* 68, 243–266. doi:10.1016/j.eurpolymj.2015.04.003

Berretta, S., Evans, K. E., and Ghita, O. R. (2016). Predicting processing parameters in high temperature laser sintering (HT-LS) from powder properties. *Mat. Des.* 105, 301–314. doi:10.1016/j.matdes.2016.04.097

Bourell, D. L., Watt, T. J., Leigh, D. K., and Fulcher, B. (2014). Performance limitations in polymer laser sintering. *Phys. Procedia* 56, 147–156. doi:10.1016/j.phpro.2014.08.157

Cebe, P., and Hong, S.-D. (1986). Crystallization behaviour of poly(ether-ether-ketone). *Polym. Guildf.* 27, 1183–1192. doi:10.1016/0032-3861(86)90006-6

Chen, P., Cai, H., Li, Z., Li, M., Wu, H., Su, J., et al. (2020). Crystallization kinetics of polyetheretherketone during high temperature-selective laser sintering. *Addit. Manuf.* 36, 101615. doi:10.1016/j.addma.2020.101615

Drummer, D., Greiner, S., Zhao, M., and Wudy, K. (2019). A novel approach for understanding laser sintering of polymers. *Addit. Manuf.* 27, 379–388. doi:10.1016/j.addma.2019.03.012

Drummer, D., Rietzel, D., and Kühnlein, F. (2010). Development of a characterization approach for the sintering behavior of new thermoplastics for selective laser sintering. *Phys. Procedia* 5, 533–542. doi:10.1016/j.phpro.2010.08.081

Dupin, S., Lame, O., Barrès, C., and Charmeau, J. Y. (2012). Microstructural origin of physical and mechanical properties of polyamide 12 processed by laser sintering. *Eur. Polym. J.* 48, 1611–1621. doi:10.1016/j.eurpolymj.2012.06.007

EOS 3D Printing Technology (2020). *How additive manufacturing works.*

Hoffman, J. D., and Lauritzen, J. I., Jr. (1961). Crystallization of bulk polymers with chain folding : Theory of growth of lamellar spherulites. *J. Res. Natl. Bur. Stand. - A. Phys. Chem.* 65, 297. doi:10.6028/jres.065A.035

Kruth, J. P., Levy, G., Klocke, F., and Childs, T. H. C. (2007). Consolidation phenomena in laser and powder-bed based layered manufacturing. *CIRP Ann.* 56, 730–759. doi:10.1016/j.cirp.2007.10.004

Leigh, D. K. (2012). "A comparison of polyamide 11 mechanical properties between laser sintering and traditional molding," in 23rd Annu. Int. Solid Free. Fabr. Symp. - An Addit. Manuf. Conf. SFF 2012, 574–605.

Mettler Toledo (2011). *Differential scanning calorimetry for all requirements*.

Motz, H., and Schultz, J. M. (1989). The solidification of PEEK. Part II: Kinetics. *J. Thermoplast. Compos. Mater.* 2, 267–280. doi:10.1177/089270578900200402

Paolucci, F., Baeten, D., Roozemond, P. C., Goderis, B., and Peters, G. W. M. (2018). Quantification of isothermal crystallization of polyamide 12: Modelling of crystallization kinetics and phase composition. *Polymer* 155, 187–198. doi:10.1016/j.polymer.2018.09.037

Paolucci, F., van Mook, M. J. H., Govaert, L. E., and Peters, G. W. M. (2019). Influence of post-condensation on the crystallization kinetics of PA12: From virgin to reused powder. *Polymer* 175, 161–170. doi:10.1016/j.polymer.2019.05.009

Stichel, T., Frick, T., Laumer, T., Tenner, F., Hausotte, T., Merklein, M., et al. (2017). A round robin study for selective laser sintering of polyamide 12: Microstructural origin of the mechanical properties. *Opt. Laser Technol.* 89, 31–40. doi:10.1016/j.optlastec.2016.09.042

Tardif, X., Pignon, B., Boyard, N., Schmelzer, J. W. P., Sobotka, V., Delaunay, D., et al. (2014). Experimental study of crystallization of PolyEtherEtherKetone (PEEK) over a large temperature range using a nano-calorimeter. *Polym. Test.* 36, 10–19. doi:10.1016/j.polymertesting.2014.03.013

Van Hooreweder, B., Moens, D., Boonen, R., Kruth, J.-P., and Sas, P. (2013). On the difference in material structure and fatigue properties of nylon specimens produced by injection molding and selective laser sintering. *Polym. Test.* 32, 972–981. doi:10.1016/j.polymertesting.2013.04.014

Van Krevelen, D. W., and Te Nijenhuis, K. (2009). Crystallisation and recrystallisation. *Prop. Polym. (Elsevier B.V.)* 19, 703–746. doi:10.1016/B978-0-08-054819-7.00019-4

Wang, Y., Beard, J. D., Evans, K. E., and Ghita, O. (2016). Unusual crystalline morphology of poly aryl ether ketones (PAEKs). *RSC Adv.* 6, 3198–3209. doi:10.1039/C5RA17110E

Yi, N., Davies, R., Chaplin, A., and Ghita, O. (2022). Novel backbone modified polyetheretherketone (PEEK) grades for powder bed fusion with enhanced elongation at break. *Additive Manufacturing* 55, 1–10. doi:10.1016/j.addma.2022.102857

Zarringhalam, H., Hopkinson, N., Kamperman, N. F., and de Vlieger, J. J. (2006). Effects of processing on microstructure and properties of SLS Nylon 12. *Mater. Sci. Eng. A* 435-436, 172–180. doi:10.1016/j.msea.2006.07.084

Zhu, W., Yan, C., Shi, Y., Wen, S., Liu, J., and Shi, Y. (2015). Investigation into mechanical and microstructural properties of polypropylene manufactured by selective laser sintering in comparison with injection molding counterparts. *Mat. Des.* 82, 37–45. doi:10.1016/j.matdes.2015.05.043